ISTITUTO NAZIONALE DI FISICA NUCLEARE

Laboratori Nazionali di Frascati

INFN-16-10/LNF
30th June 2016

Studies of geometric wakefields and impedances due to collimators

Alex Brynes[1], Giovanni Castorina[1], O. Frasciello[1], Augusto Marcelli[1;2] and Bruno Spataro[1]

[1)] *INFN-Laboratori Nazionali di Frascati Via E. Fermi 40, Frascati, Italy*

[2)] *RICMASS - Rome International Center for Materials Science Superstripes, Via dei Sabelli 119A, 00185 Roma, Italy*

Abstract

In this note we study the geometric wakefields generated by a driving electron bunch in the SPARC LAB COMB chamber. Due to the change in iris radius of the beam pipe leading into the chamber, the electron beam will induce wakefields, which can have an effect on the bunches in the train used for the SL COMB experiment. Here, we present wakefields and impedances simulations and determine the effects that they may have on the beam properties.

Pubblicato da SIDS–Pubblicazioni
Laboratori Nazionali di Frascati

1 Introduction

A new technique to produce a short train of electron bunches, which can be used in beam-driven plasma wakefield acceleration experiments has been proposed at SPARC_LAB [1]. If a significant acceleration of the witness bunch is to be achieved the requirements on the properties of the driving electron bunches are of great importance. Due to the dimensions of the plasma cavity, the beam pipe radius will change, effectively acting as a collimator. In this note, we present simulations of the geometric wakefields due to various designs of the collimator, their associated impedances and loss factors. We will then determine the effects that these wakefields will have on the electron bunches.

2 Wake potentials and loss factors

Here we will give a brief overview of how wakes, impedances and loss factors are defined for both the longitudinal and transverse cases. A more thorough treatment is given in Refs [2] and [3]. A charged particle beam travelling in a vacuum chamber can induce electromagnetic fields in the structure, which can then in turn have an effect on beam dynamics and bunch properties, particularly when the vacuum chamber presents irregularities or discontinuities. These wake fields appear behind the driving bunch (as long as $\beta = 1$, which is the case for bunches at SPARC_LAB upon emission from the RF gun). The longitudinal wake potential (in Volts) is defined as the change in voltage of a unit charge trailing behind a leading charge. If either charge has an offset from the beam pipe axis, the trailing charge can experience a transverse momentum kick, also known as the transverse wake potential (in Volts). The wake functions are defined as the wake potentials per unit charge. If we consider an electron bunch, with a charge Q, travelling through a cylindrically symmetric cavity along the z-axis it is followed by a test charge, with a charge q, at a distance s from some point in the bunch, for example the centre of the bunch. The energy change of the test charge can be calculated using the longitudinal Lorentz force, $F_{\parallel}(s, z)$ produced by the bunch:

$$U_{\parallel} = -\int_{-\infty}^{\infty} dz F_{\parallel}(s, z) \tag{1}$$

In addition, if the bunch has a transverse offset, x, from the beam pipe axis, then it can induce a transverse electromagnetic force, $F_{\perp}(s, z)$, which can affect the beam dynamics of the bunch and of any bunches trailing behind it. This transverse wake has a dependence on x in addition to s. The momentum kick experienced by a bunch with a given transverse offset is given by:

$$U_\perp = \int_{-\infty}^{\infty} dz F_\perp(s,z) \tag{2}$$

The longitudinal wake function, $W_\parallel(s)$, can have an effect also on the energy spread of the trailing charge measured as V/C. The transverse wake potential, $W_\perp(s)$, can affect the transverse emittance of the bunch and any bunches trailing behind it and it is measured as V/cm:

$$W_\parallel = \frac{U_\parallel}{Qq} \tag{3}$$

$$W_\perp = \frac{U_\perp}{Qqx} \tag{4}$$

If we consider a bunch with a longitudinal charge density $\lambda(s)$, and defining the impulse wake functions (i.e., for a point-like bunch) as $W_{\parallel 0,\perp 0}(s)$, we may also define the wake functions by using a convolution integral:

$$W_\parallel(s) = \int_0^{\infty} ds' \lambda(s-s') W_{\parallel 0}(s') \tag{5}$$

$$W_\perp(s) = \int_0^{\infty} ds' \lambda(s-s') W_{\perp 0}(s') \tag{6}$$

In the ultra-relativistic limit, due to causality the impulse wake functions will be negligible. We can also determine the total energy lost by the test charge after passing through the collimator, defined as the longitudinal loss factor $k_\parallel$. The transverse loss factor, $k_\perp$, describes the amplitude of the transverse momentum kick experienced by the trailing charge:

$$k_\parallel = \frac{U_\parallel}{q^2} \tag{7}$$

$$k_\perp(x) = \frac{U_\perp}{q^2 x} \tag{8}$$

The Fourier transform of the impulse wake functions then gives the longitudinal and transverse impedances, $Z_\parallel(\omega)$ and $Z_\perp(\omega)$

$$Z_\parallel(\omega) = \frac{1}{c} \int_0^{\infty} ds\, W_\parallel 0(s) \exp(i\omega s/c) \tag{9}$$

$$Z_\perp(\omega) = -\frac{i}{c} \int_0^{\infty} ds\, W_\perp 0(s) \exp(i\omega s/c) \tag{10}$$

We may decompose these impedances into the real and the imaginary part:

$$Z_{\parallel}(\omega) = R_{\parallel}(\omega) + iX_{\parallel}(\omega) \tag{11}$$

$$Z_{\perp}(\omega) = R_{\perp}(\omega) + iX_{\perp}(\omega) \tag{12}$$

measured as Ω and Ω/m, respectively, and behave like a regular circuit impedance in the ultra-relativistic approximation.

3 Simulation parameters

In Fig. 1 are shown some of the designs of the various collimators we considered for the SL_Comb chamber. Fig. 1(a) shows a simple collimator, where the beam pipe radius decreases sharply. Subsequent designs include tapering collimators of decreasing angles, in order to observe the effect of a smoother transition between radii. Ref [4] gives expressions for the impedances due to collimators with smooth tapering angles. The beam pipe radius for the SL_Comb chamber, b_1, is 20 mm, b_2, the final radius of the collimator, is 2.5 mm, and the collimator has a length, L, of 10 cm. Fig. 1(e) shows the structure with the smallest tapering angle of 0.41241 radians.

4 Wake Potentials and loss factors

4.1 Wake potentials

The ABCI [6] code allows the user to calculate the wake potential, impedance and loss factor, as a function of s (the distance behind the head of the bunch), of a Gaussian bunch passing through an axisymmetric structure, in both the longitudinal and transverse planes. A variable radial mesh can be implemented for cases where the radius of the beam pipe changes. The sizes of the mesh in both r and z directions allows for fast, accurate computation. By using Napoly's integration method [7], the calculation can be performed with beam pipes which are short at both ends.

We also determined the transverse wake potential as a function of the tapering angle. Plots corresponding to $W_{\parallel}$ and $W_{\perp}$ for the cavities shown in Fig.1(a e) are given in Figs.2 and 3. We see that as the tapering angle decreases, the peak of the transverse wake potential decreases, as this allows for a smoother transition down to the smaller beam pipe radius.

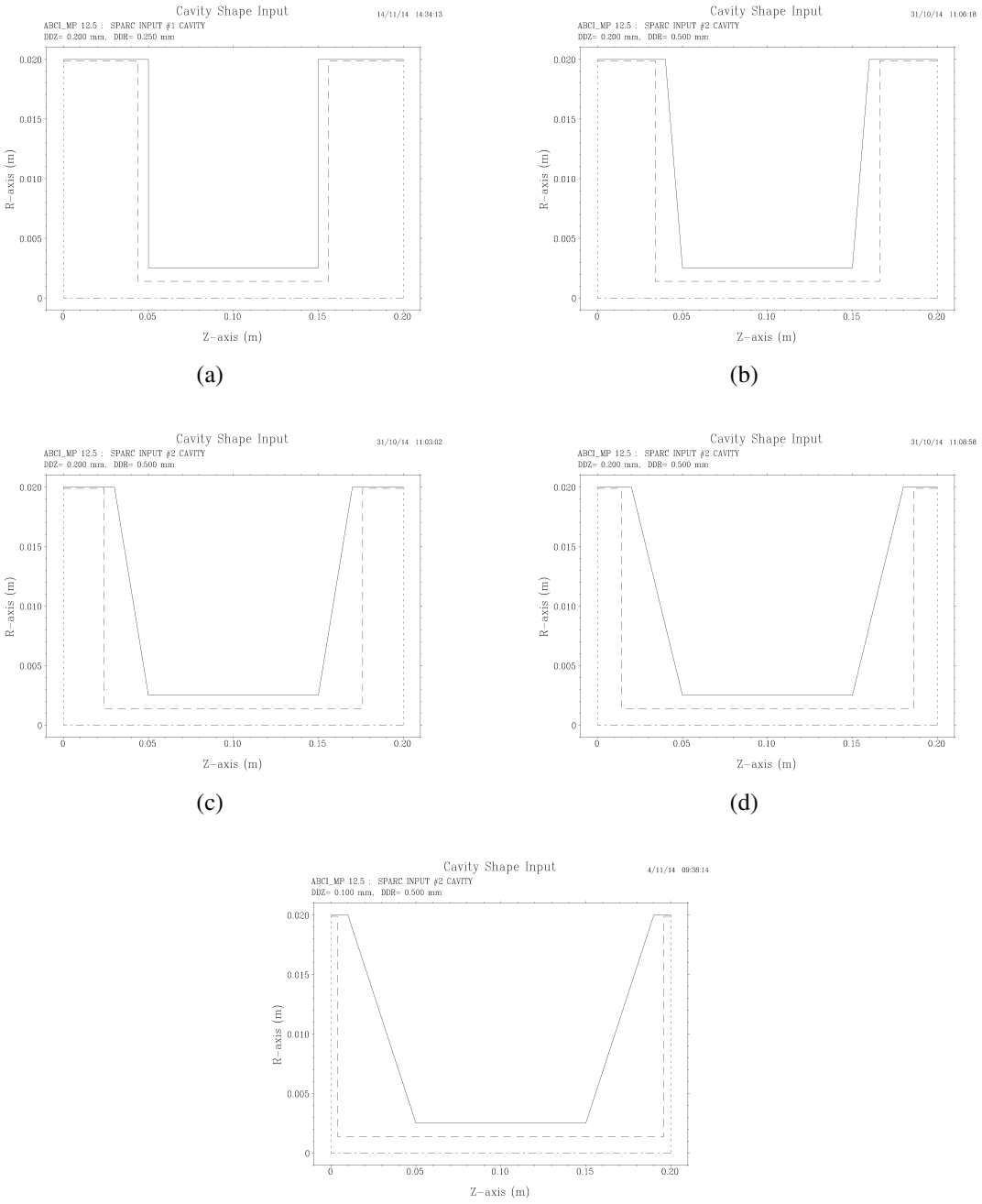

Figure 1: Collimator designs used for ABCI simulations. All collimators are axisymmetric

4.2 Loss factors

In terms of the effects of the longitudinal wakes on the properties of the bunch, the integrated longitudinal wake potential is probably the most significant parameter, as this

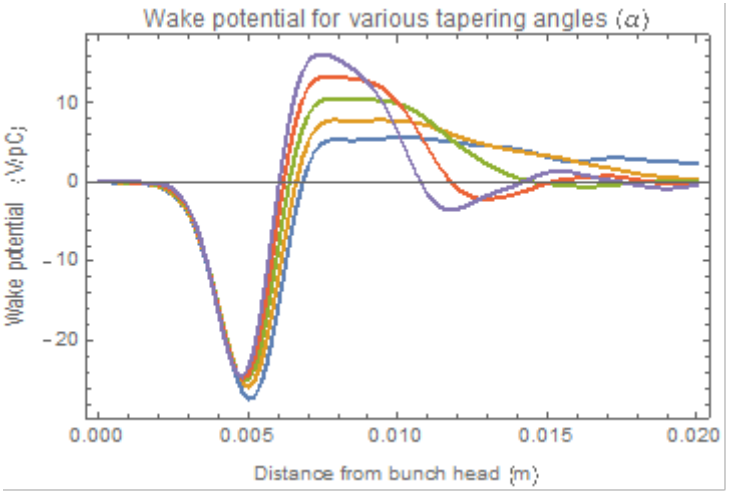

Figure 2: The Wake potential (in V/pC) as a function of the tapering angle

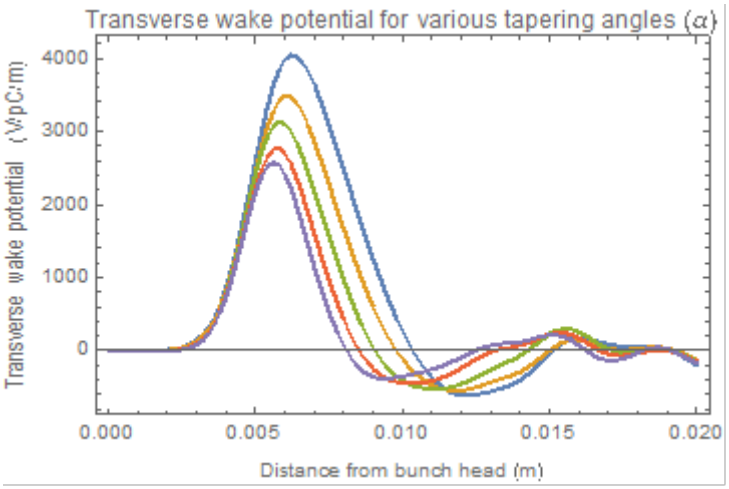

Figure 3: The transverse wake potential as a function of the tapering angle

gives the total energy loss of the test charge. We allowed the beam pipe length to vary and calculated the longitudinal loss factors for the cavities in Fig. 1(a) and 1(e) as we expected to see the largest variations between these two cavities (see Fig.4a and 4b).

As the beam pipe length is extended, the levelling off of the loss factor is expected. As the length becomes sufficiently long, the wake fields behind the bunch will become negligible. In order to observe the trend of how both $k_{\|}$ and $k_{\perp}$ depend on the tapering angle, we listed these values in Table 1. Data clearly show that both loss factors decrease as the tapering angle decreases.

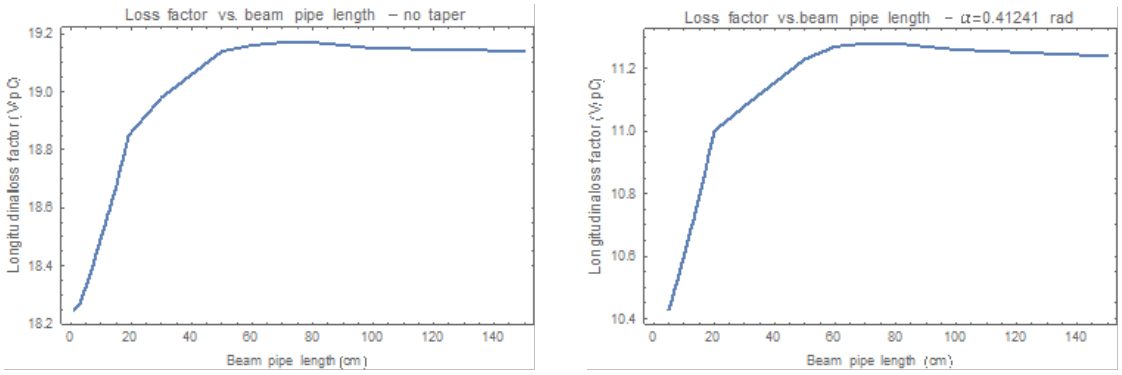

(a) (b)

Figure 4: Longitudinal loss factor (in V/pC) as a function of beam pipe length for the collimators in Figs. 1(a) and 1(e)

Table 1: $k_{\|}$ and $k_{\perp}$ as a function of for a beam pipe 50 cm long

Tapering Angle	$k_{\|}$ (V/pC)	$k_{\perp}$ (V/pC/mm)
$\alpha = \pi/2$	19.11	2.493
$\alpha = 1.05165$	17.32	2.241
$\alpha = 0.71883$	15.25	2.042
$\alpha = 0.528074$	13.19	1.842
$\alpha = 0.41241$	11.23	1.703

5 Effects on the beam

5.1 Kick factors

As previously mentioned, the longitudinal wakefields can increase the energy spread of the electron bunch. Various schemes have been suggested [5] which, depending on the geometry under consideration, can generate analytical formulae which are useful for our purposes. The so-called diffraction regime is appropriate when:

$$\frac{kb_2}{L} \gtrsim j_{01}^2 \tag{13}$$

Where $k = \frac{\omega}{c}$ and j_{01}^2 is the first root of the Bessel function J_0. For $\omega \geq 50\,GHz$, this condition holds. It has been shown that in the diffraction regime, the longitudinal impedance of a round step collimator at high frequency can be given as:

$$Z_{\|,HF} = \frac{Z_0}{\pi} ln(\frac{b_1}{b_2}) \tag{14}$$

Approximate values for the longitudinal loss factor and the wakefield-induced energy spread for a Gaussian bunch in the high frequency limit can be estimated [8]:

$$k_{\parallel,HF} = \frac{c}{2}\frac{Z_{\parallel,HF}}{\sqrt{\pi}\sigma} \tag{15}$$

$$k^{rms}_{\parallel,HF} = \sqrt{\int_{-\infty}^{+\infty} ds\lambda(s)[W_{\parallel}(s) - k_{\parallel,HF}]^2} \approx 0.4k_{\parallel,HF} \tag{16}$$

Considering the values of our geometry we estimated $k_(\ \parallel, HF) \approx 21.11\ V/pC$, and thus the energy spread $k^{rms}_{\parallel,HF} \approx 8.4\ V/pC$. The ABCI simulations give a value of $k_{\parallel} = 19.11\ V/pC$ for the cavity shown in Fig.1(a). For the SL_COMB experiment, the bunch charge should not exceed 50 pC, giving a wakefield-induced energy spread of 400 V. For a beam energy of 120 MeV, the energy spread is negligible. Moreover, as we are in the diffractive regime, we can also assume that the beam pipe is relatively long. In this way, if it has an offset from the beam pipe axis we may obtain the transverse momentum kick that the beam may experience. Assuming that our collimator is long ($L \sim a^2/\sigma$) we can calculate the transverse impedance:

$$Z_{\perp,HF} = \frac{Z_0 c}{\omega\pi}\left(\frac{1}{b_2^2} - \frac{1}{b_1^2}\right) \tag{17}$$

From the value of $Z_{\perp}$, we can calculate the transverse kick factor and the induced momentum spread of a Gaussian bunch:

$$k_{\perp,HF} = \frac{\omega}{2}Z_{\perp} \tag{18}$$

$$k^{rms}_{\perp,HF} = \frac{k_{\perp,HF}}{\sqrt{3}} \tag{19}$$

Giving an estimate for the high-frequency transverse kick factor of $k_{\perp,HF} \approx 5.66\ V/pC/mm$, the induced momentum spread due to this kick is $k^{rms}_{,HF} \approx 3.29\ V/pC/mm$. We can also compare the above numerical results with analytical results regarding the imaginary part of the transverse impedance at zero frequency [9]. The transverse loss factor, $k_{\perp}$, is related to the imaginary part of the transverse impedance at zero frequency in the following way:

$$X_{\perp}(\omega = 0) = -\frac{2\sqrt{\pi}\sigma}{c}k_{\perp} \tag{20}$$

As an example, the numerical value calculated for the cavity 1(e) is $X_{\perp}(\omega = 0) = 19.583\ k\Omega/m$. The transverse loss factor is 1.703 kV/pCm, and thus we obtain $Im[Z_{\perp}(\omega = 0)] = 20.137\ k\Omega/m$. Since the code is within 3% of the analytical value we can consider the numerical results accurate enough for our purposes. We also find that the transverse loss factor is approximately 25% larger for the step collimator.

5.2 Transverse emittance growth

In order to determine the effects that the collimator wakefields may have on the transverse phase space of a real beam, we can calculate the mean centroid kick given to a bunch with an offset from the beam axis x. This kick is then given by [10]:

$$\theta = \frac{xQk_{\perp}^{avg}}{E} \tag{21}$$

Where Q is the bunch charge, $k_{\perp}^{avg}$ is the transverse kick factor averaged over the length of the beam, and E is the energy of the beam. For the SL_COMB experiment, the driving bunches have a charge of 50 pC, and the witness bunch has a charge of 25 pC, all with $E = 120MeV$. We can then determine the transverse emittance growth due to this kick:

$$\epsilon_x = \sqrt{\left(\epsilon_{x;0}^2\left(1 + \frac{\beta_x}{\epsilon_{x;0}}\theta^2\right)\right)} \tag{22}$$

where $\epsilon_{x,0}$ is the x-emittance at the entrance of the collimator, ϵ_x is the x-emittance after the kick, and β_x is the betatron function at the entrance of the collimator. ABCI gives a value of $k_{\perp}^{avg} = 2.453\ V/pC/mm$. If we estimate $\epsilon_{x,0} = 1\ mm\,mrad$, $\beta_x = 10$ m and an offset in x of 1 mm, a negligible emittance growth for all collimator designs is obtained.

6 Collimator with a capillary

6.1 Perfectly conducting capillary

We have also considered a layout with a short capillary within the collimator with the aim of studying the effects of the beam passing through a dielectric material. Our initial ABCI studies were limited to characterize the behaviour of geometric wakefields of a perfectly conducting structure. Below are presented some of our results. The geometries of cavities 1(a) and 1(e) were modified to include capillaries of different radii: 500 m, 750 m and 1000 m, in the centre of the collimators, with a length of 2 cm (see Fig.5). We calculated that the longitudinal loss factors are largely unchanged when a capillary is included in the geometry, but $Z_{\parallel}$ and $Z_{\perp}$ are around an order of magnitude larger than in the initial designs. If we assume that the Equation (15) is still valid (which may not be the case, due to the more complex geometry), we first determine if our simulations are giving reasonable values. A comparison between the numerical values of $X_{\perp}(\omega = 0)$ and that obtained using the Equation (15) is given in Table 2.

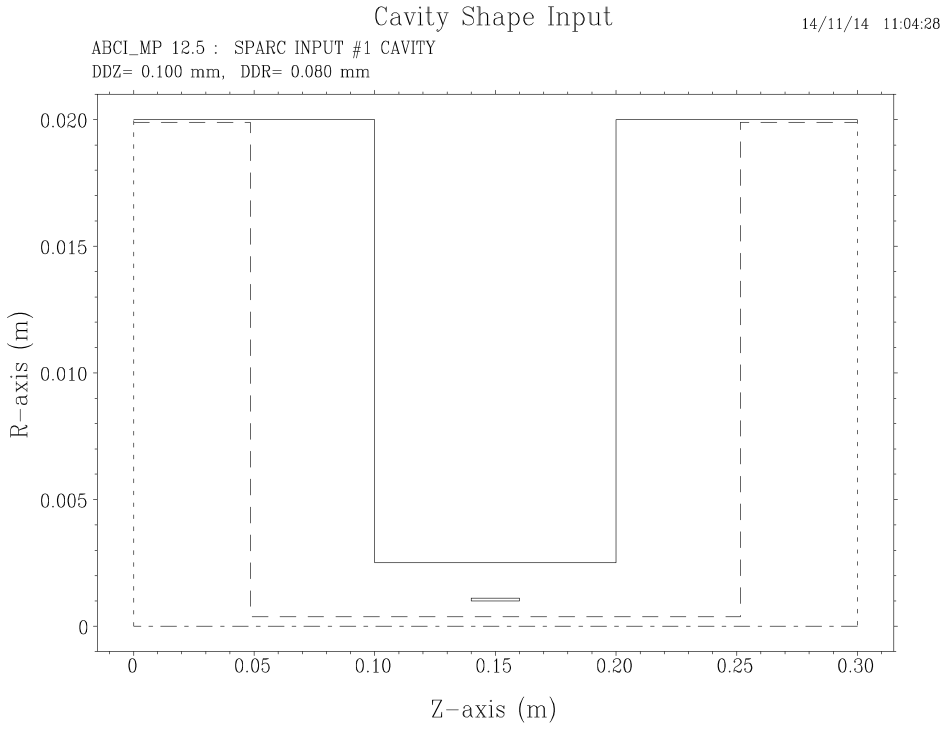

Figure 5: Schematic of the step collimator in Fig.1(a) with a short capillary included in the geometry.

We can consider these numerical values sufficiently accurate for our purposes. Fig.6 gives plots of $Z_{\parallel}$ and $Z_{\perp}$ for the three capillary radii given above. The impedances for the geometries with capillary radii of 750 μm and 1000 μm appear to level off or decrease in the high-frequency limit, but the geometry with a capillary radius of 500 μm continues to increase. In order to check the validity of these simulations, we did a cross-check with the 3-D EM code GdfidL [11]. Simulations run for the same geometry with a capillary radius of 500 μm, both with a perfectly conducting capillary and with an aluminium capillary. Results for impedances and wake potentials for this geometry as generated by both codes are given in Fig.7. We can see that both codes match up quite well. Discrepancies between the two sets of simulations may be due to a difference in the mesh sizes. It was also determined that the resistive wakes due to the aluminium capillary have a small effect in comparison with the geometric wakes.

Table 2: Comparison between analytical and numerical calculations of $X_\perp(\omega = 0)$, $[k\Omega/m]$

Capillary Radius	500 μm	750 μm	1000 μm
ABCI	320.92	197.06	140.12
Analytical	308.38	184.35	152.86
% difference	4	6	8

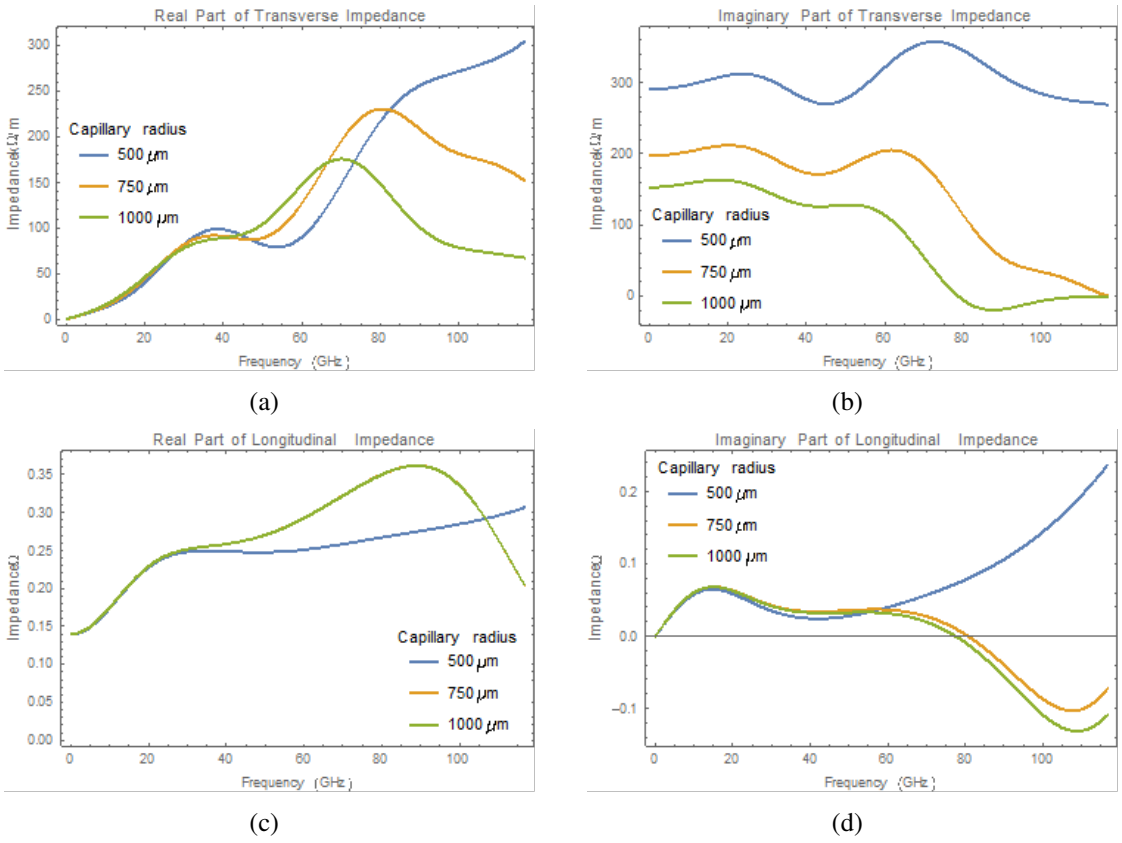

Figure 6: $Z_\parallel$ and $Z_\perp$ for various capillary radii, as computed by the ABCI code

6.2 Dielectric capillary

A modified version of the ABCI code allows the user to include dielectric materials in their simulations [12]. The inclusion of a dielectric material can induce trapped modes, which give rise to resonances in the impedance of the structure. We have simulated the impedances in the structure shown in Fig. 5 for a range of dielectric constants for the capillary.

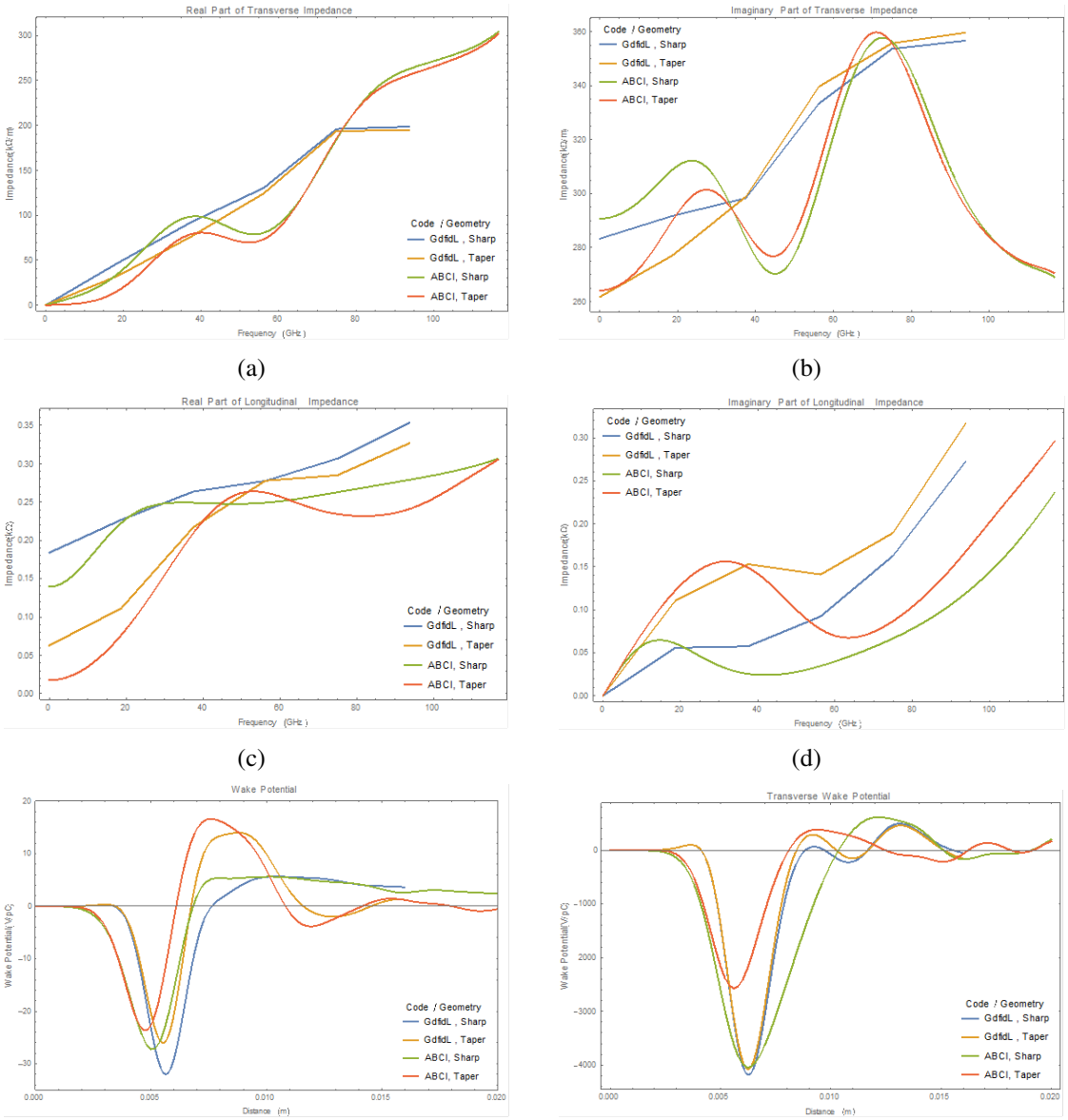

Figure 7: $Z_{\parallel}$, $Z_{\parallel}$, $W_{\parallel}$ and $W_{\perp}$ as computed by the GdfidL and ABCI codes, for a perfectly conducting capillary

7 Conclusions

We have simulated the longitudinal and transverse wakefields and impedances due to different designs of collimators for the SL_COMB chamber. By analysing various tapering angles, we have determined that both the longitudinal and transverse loss factors become smaller as the tapering angle decreases. Our numerical results calculated using the ABCI

code, correspond reasonably well with analytical formulae. It allows to determine the effect that these wakefields will have on the bunches used in the SL_COMB experiment. It is expected that, unless the beam has a large offset from the axis of the beam pipe, these wakefields will significantly affect the beam.

We have also considered a modified geometry in which a thin capillary is inserted inside the beam pipe. Initially, our simulations were run using both ABCI and GdfidL for a perfectly conducting capillary. The results of both codes for the real and imaginary parts of the longitudinal and transverse impedances in this structure were found to match up reasonably well for both codes, as did the wake potentials. In GdfidL an aluminium capillary was also considered, and we determined that the resistive wakes did not have a large impact on the total wakes generated. By using a modified version of the ABCI code, which allows the user to include dielectric structures in the geometry, we were also able to simulate the resonances in the impedance of capillaries with various dielectric constants.

As a final comment the CST software [13] gave a similar transverse kick estimation.

References

[1] A. Mostacci et al, Proc. of IPAC 11, THYB01 (2011)

[2] K. L. F. Bane, P. B. Wilson, T. Weiland, *Wake Fields and Wake Field Acceleration*, SLAC-PUB-3528 (1984)

[3] L. Palumbo, V. G. Vaccaro, M. Zobov, *Wake Fields and Impedance*, LNF-94/041 (1994)

[4] K. Yokoya, *Impedance of Slowly Tapered Structures*, CERN SL-90-88 (1990)

[5] G. V. Stupakov, *Impedance of Small-Angle Collimators in High-Frequency Limit*, SLAC-PUB-8857 (2001)

[6] ABCI Code, `http://abci.kek.jp/`

[7] O. Napoly, Y. H. Chin, B. Zotter, *A Generalized Method for Calculating Wake Potentials*", Nucl. Instrum. Methods, A334, 255 (1993).

[8] M. Dohlus, I. Zagorodnov, O. Zagorodnova, *Impedances of Collimators in European XFEL*, TESLA-FEL 2010-04 (2010)

[9] G. V. Stupakov, *Geometrical Wake of a Smooth Taper*, SLAC-PUB-7086 (1995)

[10] J. Resta-Lpez, *Single-bunch Transverse Emittance Growth due to Collimator Wake-field Effects*, http://arxiv.org/pdf/1309.0480.pdf (2013)

[11] GdfidL Code, `http://www.gdfidl.de/`

[12] Y. Shobuda, Y. H. Chin, K. Takata, *Impedance of a Ceramic Break and its Resonance Structures*, PR-STAB 17, 091001 (2014)

[13] CST Code, `https://www.cst.com/`